Research Article

International Journal of Advanced Technology and Engineering Exploration, Vol 12(125)
ISSN (Print): 2394-5443 ISSN (Online): 2394-7454
http://dx.doi.org/10.19101/IJATEE.2024.111101175

Design and analysis of a polder system for urban flood control: a case study of the Bendung sub-catchment, Palembang City

Marlina Sylvia[1], Anis Saggaff[2*] and F.X. Suryadi[3]
Research Scholar, Department of Civil Engineering and Planning, Faculty of Engineering, Universitas Sriwijaya, Indralaya, Indonesia, 30662[1]
Department of Civil Engineering and Planning, Faculty of Engineering, Universitas Sriwijaya, Indralaya, 30662, Indonesia[2]
Water and Agriculture Core, IHE Delft Institute for Water Education, Delft, The Netherlands[3]

Received: 04-July-2024; Revised: 25-March-2025; Accepted: 08-April-2025

Abstract
This research proposed the implementation of a polder system to protect the Bendung sub-catchment of Palembang City from inundation and flooding. The system consists of several key components, including ring dikes, outlet structures, and storage areas such as drainage canals and retention basins. The results indicate that the polder system is a viable option for flood protection in the Bendung sub-catchment, utilizing outlet structures, ring dikes, and temporary storage facilities. The existing pumping system, with a total capacity of 18 m^3/s, was found to be sufficient for controlling water levels in the lower part of the polder when operated systematically. The duFlow program was used for the analysis, modeling both steady and unsteady flow, as well as water quality processes in one-dimensional open channel systems. Hydraulic response analysis revealed that only three pump units, each with a capacity of 9 m^3/s, were needed to effectively regulate the water level in the lower area. However, to address water level management in the upper part and account for land use within the river plain, constructing a dike system along the river is recommended over river normalization. Expanding river profiles, particularly in areas already densely occupied by residential structures, was deemed infeasible.

Keywords
Urban flood control, Polder system, Bendung sub-catchment, Hydrodynamic modelling, Flood mitigation, duFlow simulation.

1.Introduction
Palembang City, located in the lowland area of South Sumatra, is highly prone to flooding, particularly influenced by the Musi River and its tributaries, including the Bendung River [1, 2]. Each rainy season, the city faces increasingly complex flood problems, mainly driven by rapid urbanization, land-use changes, and the rising frequency of extreme weather events [3]. Palembang's topographical elevation, ranging from 0 to 20 meters above sea level, exacerbates the risk of flooding and waterlogging in urban areas. To address these issues, the Palembang City Government, in collaboration with the Ministry of Public Works and Housing, has undertaken various flood mitigation efforts. One of the promising solutions considered is the implementation of a polder system, a flood control mechanism proven effective in lowland urban areas.

A polder system manages rainwater and surface runoff using infrastructures such as ring dikes, drainage canals, retention basins, and pumping systems [4, 5].

However, implementing a polder system in the Bendung sub-catchment faces considerable challenges. The primary constraint is the limited space available for constructing polder components due to extensive urban development. Additionally, community participation and institutional support are critical to ensuring the long-term sustainability of such systems [6].

Previous studies have demonstrated that integrating surface water and groundwater models enhances flood prediction accuracy and supports more effective infrastructure planning [7, 8]. Given the low elevation, rapid urbanization, and vulnerability to extreme rainfall and tidal surges, the Bendung sub-

*Author for correspondence

catchment offers an ideal case study for exploring polder-based flood management [9, 10].

This research aims to assess the feasibility and effectiveness of a polder system in controlling urban floods in the Bendung catchment area. Technical, environmental, and social aspects are considered to provide strategic recommendations for sustainable urban drainage planning. The methodology includes a literature review, hydrological and topographical data collection, hydrodynamic modeling using the duFlow program, and an evaluation of the polder system's performance under various scenarios. It also accounts for the effects of climate change, including changes in rainfall patterns and sea-level rise, and explores the role of real-time monitoring and adaptive flood control technologies to enhance future system resilience. This study aspires to contribute to the development of a sustainable, climate-adaptive flood management framework for Palembang City.

The paper is organized as follows: the literature review is presented in Section 2, followed by materials and methods in Section 3. The results and discussion are illustrated and analyzed in Section 4, and the paper concludes with Section 5.

2.Literature review

Palembang City has long struggled with recurring floods, attributed to its geographical location within the floodplain of the Musi River and its sub-basins, including the Bendung River [1, 2]. Rapid urbanization, land-use changes, and intensifying extreme weather events have further exacerbated the city's flood vulnerability [3].

Urban flood management in similar lowland areas has increasingly favored the adoption of polder systems. A polder is an artificial hydrological unit surrounded by ring dikes, with controlled discharge through outlets (gravity or pumping systems) [4]. The polder system ensures that groundwater and surface water levels are managed independently of surrounding hydrological conditions, thus optimizing water management within enclosed zones [5].

The operational principles in tertiary blocks include:

- Water discharge and soil washing management,
- Controlled drainage,
- Sub-irrigation through seepage channels, and
- Tidal irrigation adaptation [6].

Studies emphasize that integrating surface water and groundwater models significantly improves flood forecasting accuracy, benefiting flood control planning [7, 8]. However, implementing polder systems in heavily urbanized regions like the Bendung sub-catchment faces challenges such as the scarcity of available land for constructing essential components like drainage canals, retention basins, and pumping stations [11, 12]. Community engagement and institutional backing are vital for ensuring operational sustainability [13].

Key characteristics of polder systems include [14]:

1. No inflow of foreign water except from rain, seepage, or controlled irrigation,
2. Controlled discharge through designated outlet structures,
3. Artificial maintenance of groundwater and surface water levels within the polder.

In Palembang, the existing nine sub-drainage systems can conceptually function as individual polders [9]. Given the low-lying geography, gravity drainage is feasible only when the external water level is lower than the polder ground level. Otherwise, pumping systems must be employed to manage water levels effectively [15, 16].
Lessons from other Indonesian regions highlight the importance of:

- Regular maintenance of drainage networks,
- Sediment control to prevent blockages, and
- The use of automated systems for enhanced operational efficiency [17, 18].

Recent advancements include the integration of IoT-based real-time flood monitoring and automated pumping stations, which significantly enhance polder system responsiveness and cost-efficiency [19–21]. Additionally, renewable energy technologies, such as floating solar panels, have been suggested for powering polder pumping stations, offering a sustainable and eco-friendly alternative to conventional energy sources [22–24]. The methodology typically applied for polder design and evaluation includes problem analysis, data collection (topography, hydrology, land use, water levels, tides), scenario development, hydrodynamic modeling, and system performance analysis [21–23]. Based on these considerations, the components of a polder system are shown in *Figure 1* [21]. The future success of polder systems in flood-prone urban areas like Palembang depends on the integration of adaptive management strategies and climate resilience measures, particularly considering the projected impacts of sea-level rise and intensified precipitation events.

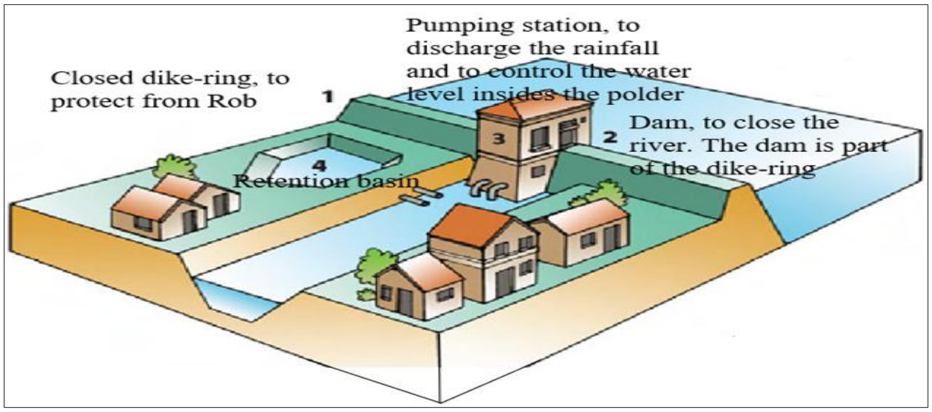

Figure 1 Components of a typical polder system: ring dikes, drainage canals, retention basins, and outlet structures

3.Materials and methods

The data used in this research consisted of primary and secondary sources. Primary data were collected through field observations, including measurements of channel dimensions, surface and channel bed topography, and tidal data in rivers using a measuring board. Direct observations were conducted over three visits during the rainy season to ensure accurate flood data collection. Flood heights were measured using a millimeter-scale measuring board placed at several key inundation points. Flow discharge was recorded using a flow meter at selected strategic locations. River tide data were gathered through the installation of an automatic recording device operating continuously for 24 hours to capture water level fluctuation patterns.

Secondary data included rainfall records obtained from the Badan meteorologi, klimatologi, dan geofisika (Meteorology, Climatology, and Geophysics Agency) (BMKG), flood location data, and topographic maps sourced from the Palembang City Public Works Department. Rainfall data from BMKG were analyzed using the Thiessen polygon method. Flood point location data and topographic maps were utilized to support hydrodynamic modeling and spatial analysis. Two methods were used in this research: field observation and numerical analysis. Field observations revealed numerous locations experiencing waterlogging; however, only the inundation points with sufficiently large areas were selected for further analysis. Selection was based on conditions at five channel sections along the Bendung River, considering inundation extent, surface elevation, waterway access, and the availability of pumps. In this study, river water flow analysis was conducted using the duFlow program application. The research location is the Bendung River in Palembang City. *Figure 2* shows the study area selected for numerical analysis. The inundation locations for each channel are as follows:

- **Channel 1**: STA 1+800–2+000 (veteran pump area), STA 2+400–2+600, STA 3+000–3+200, STA 3+200–3+400, and STA 4+400–4+600.
- **Channel 2**: STA 0+400–0+600 and STA 1+000–1+400 (regional police crossing area).
- **Channel 3**: STA 0+000.
- **Channel 4**: STA 0+000–0+200 and STA 0+400–0+600.
- **Channel 5**: STA 1+600 (upstream), STA 0+600–0+800, STA 0+800–1+000, and STA 1+200–1+400.

Channel topography data were obtained from the Palembang City Public Works Department, including historical records of water levels and channel elevations for the Bendung River. Additional topographic surveys were conducted specifically at points experiencing the most severe inundation. The study area lies within a tropical climate zone, characterized by high rainfall even during the dry season (May to September) and even greater precipitation during the rainy season (October to April). *Table 1* presents a recapitulation of regional rainfall analysis results using the Thiessen method, while the maximum average rainfall curve is shown in *Figure 3*. *Figure 4* illustrates the model setup procedure used in the duFlow program, and *Figure 5* provides the topographic map of Palembang City. A hydrograph represents the relationship between flow parameters and time. In the planned rainfall analysis, estimating the design flood discharge requires inputting the design rainfall into the watershed model. The design discharge was calculated using the rational method based on point rainfall depth to determine peak discharge [25]. Rainfall intensity values are summarized in *Table 2.*

Table 1 Recapitulation of regional rainfall analysis results

Year / Month	1	2	3	4	5	6	7	8	9	10	11	12
2016	54,56	76,59	68,70	49,09	49,66	34,99	24,86	70,10	91,83	59,72	61,75	74,80
2017	44,11	55,29	68,92	70,10	88,46	50,76	25,43	36,36	26,92	70,54	55,41	81,51
2018	31,83	46,72	103,97	59,46	32,25	62,70	42,47	12,81	78,43	60,51	85,47	56,53
2019	36,42	75,45	76,36	61,02	27,72	37,18	53,48	2,18	32,78	44,92	25,57	99,00
2020	43,63	78,43	79,80	81,66	78,44	46,46	28,60	49,01	28,64	64,65	73,21	52,99

Table 2 Rainfall intensity

t (jam)	R24 (m/dt) R2 (m/dt) 91,9	R5 (m/dt) 101,5	R10 (m//dt) 107,9	t (jam)	R24 (m/dt) R2 (m/dt) 91,9	R5 (m/dt) 101,5	R10 (m//dt) 107,9
0	0	0	0				
1	31,894	35,212	37,448	**13**	0,000	0,000	0,000
2	6,971	7,696	8,185	**14**	0,000	0,000	0,000
3	1,163	1,284	1,365	**15**	0,000	0,000	0,000
4	0,160	0,177	0,188	**16**	0,000	0,000	0,000
5	0,019	0,021	0,022	**17**	0,000	0,000	0,000
6	0,002	0,002	0,002	**18**	0,000	0,000	0,000
7	0,000	0,000	0,000	**19**	0,000	0,000	0,000
8	0,000	0,000	0,000	**20**	0,000	0,000	0,000
9	0,000	0,000	0,000	**21**	0,000	0,000	0,000
10	0,000	0,000	0,000	**22**	0,000	0,000	0,000
11	0,000	0,000	0,000	**23**	0,000	0,000	0,000
12	0,000	0,000	0,000	**24**	0,000	0,000	0,000

t (jam): It stands for time (in hours). "Jam" is the Indonesian word for "hour." It represents the elapsed time during a 24-hour rainfall event.
R24 (m/dt): It refers to 24-hour cumulative rainfall intensity in meters per hour (m/hour or m/dt). (It is unusual to use "m/dt" exactly, but in your context, "dt" is just referring to a unit of time, meaning per hour.), R2 (m/dt), R5 (m/dt), R10 (m/dt): These represent the rainfall intensities for different return periods. R2: Rainfall intensity corresponding to a 2-year return period (i.e., rainfall event likely to occur once every 2 years).
R5: Rainfall intensity for a 5-year return period. R10: Rainfall intensity for a 10-year return period. R2 return period = 91.9 mm/24 hours. R5 return period = 101.5 mm/24 hours. R10 return period = 107.9 mm/24 hours.

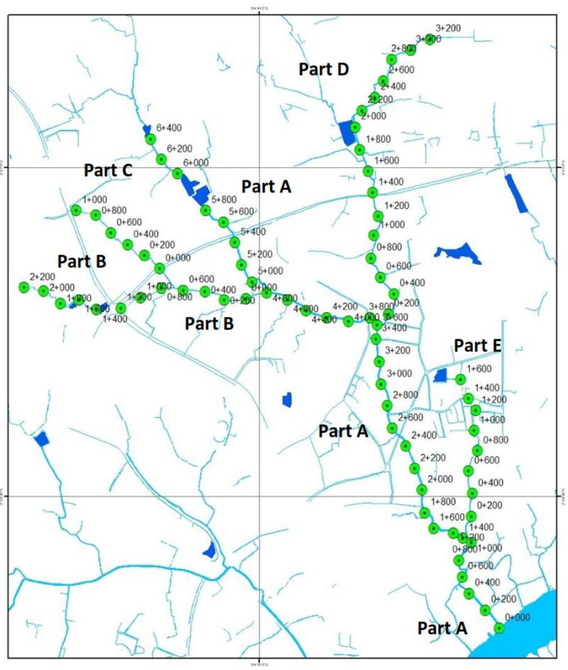

Figure 2 Channel network area of the Bendung River sub-catchment

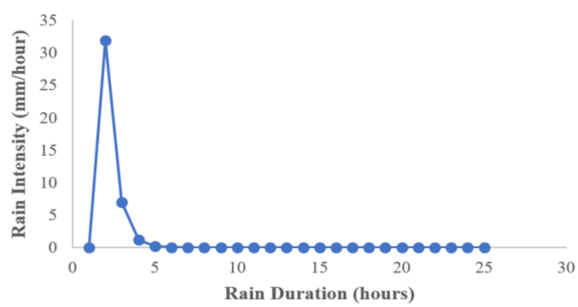

Figure 3 Maximum average rainfall curve based on rain duration

After obtaining the rainfall intensity results, the data were used to construct an intensity-duration-frequency (IDF) curve based on the Mononobe method, as shown in *Figure 6*. Although rainfall analysis initially indicated a maximum intensity of 107.9 mm for a 10-year return period, actual recorded rainfall reached 188.7 mm. This intensity corresponds to an estimated return period of 100 to 150 years. Given this anomaly, the rainfall intensity of 188.7 mm was selected for further analysis.

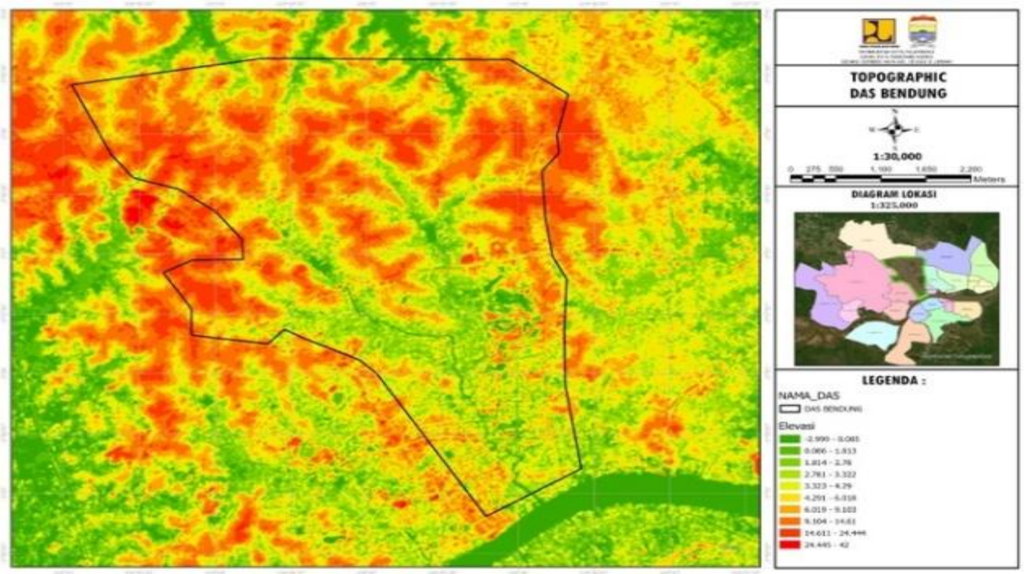

Figure 4 Topographic map of the Bendung sub-catchment in palembang city

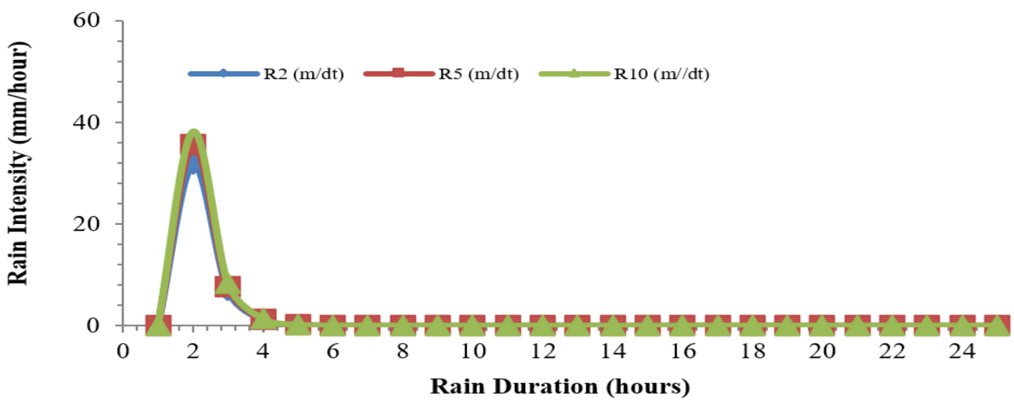

Figure 5 IDF Curves Using the Mononobe method

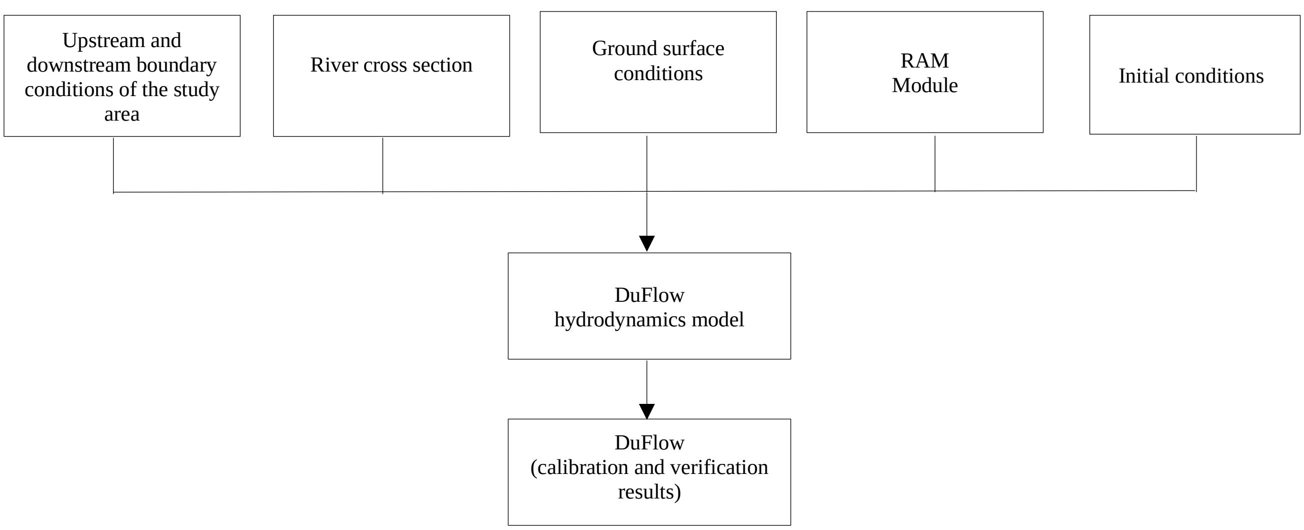

Figure 6 Set-up models used in DuFlow

In this study, hydraulic analysis was conducted using the Chezy method to evaluate flow characteristics in open channels under varying discharge conditions. The objective was to determine the Manning's roughness coefficient and the Chezy coefficient for these conditions. These coefficients were calculated using the Chezy equation (Equation 1), which is applied to assess flow velocity and resistance in open-channel hydraulics.

$$V = C.\sqrt{R.S} \quad (1)$$

Where:
V = flow velocity (m/s)
C = Chezy coefficient ($m^{1/2}/s$)
R = hydraulic radius (m)
S = slope of the channel (dimensionless)

Additionally, Manning's equation was applied to estimate flow velocities, and is presented as Equation 2:

$$V = \frac{1}{n}.R^{2/3}.\ S^{1/2} \quad (2)$$

Where n is Manning's roughness coefficient, which represents the resistance to flow due to surface roughness and channel irregularities. The methodology employed in this study involves the construction of a physical model of the channel using fiber material. The flow within the model was regulated by maintaining a constant channel slope of 0.01 and applying varying discharges of 0.0025, 0.0020, and 0.0015 m^3/s. Following the measurement and calculation of the hydraulic coefficients, these values were utilized to simulate flow conditions within the duFlow model. Subsequent duFlow simulations were conducted to analyze flood-prone locations along the Bendung River, offering insights into the river's behavior under different flow scenarios. The duFlow modeling process in this study followed a systematic approach. First, a model schematic was created within the duFlow program. Next, channel sections were defined by inputting cross-sectional data, including channel width, depth, and topography, from upstream to downstream. Rainfall data, tidal data, and the roughness coefficient (Chezy value) were also incorporated. After all parameters were entered, the simulation was executed. If the model status indicated a successful calculation, the simulation results were considered valid for further analysis. The criteria for selecting significant flood locations were based on the presence of substantial inundation with the potential to impact critical infrastructure, access points, and residential areas. Inundation areas were identified through field observations and visual assessments conducted during rainfall events.

Field data collection methods included measuring water depth using graduated measuring boards, recording flow discharge with flow meters, and utilizing GPS devices for precise location tracking. Photographic documentation was also performed at each site to capture inundation conditions and support further analysis.

4.Results and discussion

In certain cases, a combination of a gravity outlet and a pumping system is utilized, particularly to facilitate the flushing of the system during low tide conditions. This combination helps maintain the balance of water levels while optimizing drainage efficiency. Adjacent to the pumping station in the Bendung polder area, a gravity outlet is also provided, as shown in *Figure 7*. A hydrodynamic model was employed to simulate various scenarios of the polder water management system, using the Saint-Venant equations for continuity and momentum analysis. This model aids in understanding the behavior of water flow and the interactions between system components, including pumps, gravity outlets, and drainage canals.

Figure 7 Gravity outlet and pumping system at the Bendung river mouth

Ring dikes and collector drain

In the Bendung area, the implementation of ring dikes appears feasible, as shown in *Figure 3*, since most of the proposed dike alignments follow existing roadways of sufficient structural integrity. However, an essential consideration is the verification of crest elevation to ensure protection against runoff from external areas. As the polder functions as a closed hydrological system, collector drains must be constructed alongside the ring dikes to store runoff originating within the polder boundaries [26].

Gravity outlet and pumps

According to hydrodynamic model simulations, the currently installed pumping station at the mouth of the Bendung River, with a capacity of 36 m^3/s, is sufficient to manage runoff within the Bendung sub-catchment. This supports the recommendation that the optimal location for a pumping station is at the lowest point of a polder. In this case, the Bendung pumping station is strategically located near the Musi River. Additionally, the gravity outlet must be regularly maintained, as it plays a crucial role during low tides for water drainage and flushing operations.

Drainage canals

Drainage canals are already present throughout the Bendung area and have been maintained by the Palembang City Public Works Department. The hydrodynamic simulation emphasizes the importance of regular maintenance, including solid waste management, to prevent blockages that can lead to flooding. The system's efficiency can be significantly enhanced through consistent monitoring and the implementation of operation and maintenance guidelines. Encouraging community participation is also essential; public awareness and individual responsibility are key to sustainable flood management.

Polder as a closed system and no open connection with an outside water body

In the Bendung polder system, a gravity outlet is proposed to facilitate the flushing of poor-quality water into the Musi River during low tide conditions. However, it is essential to emphasize that under normal flow conditions, especially during the rainy season when active pumping is required for drainage, the gravity outlet must remain closed. Failure to do so would result in an open connection between the polder and the Musi River, thereby compromising the closed-system integrity of the polder. In such a scenario, water that has been pumped out may re-enter the polder, creating inefficiencies and potential flood risks [26].

To mitigate this risk, the installation of a flap gate is recommended in place of a conventional sliding gate. A flap gate can automatically prevent backflow during high external water levels while allowing discharge during low tide without manual intervention. An integrated management approach should be adopted [27], considering both technical factors (e.g., hydrodynamic performance, sediment and solid waste control) and non-technical aspects (e.g., institutional coordination and community engagement in flood management).

Additionally, routine inspections and functional assessments of all gate mechanisms are crucial to ensure they operate as intended, particularly during high-water or emergency events. Ensuring proper gate functionality is vital to maintaining the effectiveness and resilience of the polder system.

Water management board for polder Bendung

Given the complexity of the Bendung polder system, it is recommended that a dedicated Water Management Board be established. This board should comprise key stakeholders, including the River Basin Authority, the Department of Public Works and Public Housing of Palembang City, and representatives from the local communities residing within the Bendung polder area. Its primary mandate would be to oversee the day-to-day operation and management of the water infrastructure, taking into account both technical and non-technical considerations.

In addition to operational oversight, the board would serve as a central body for ensuring effective coordination and communication between local and external water management agencies. Active participation from community representatives is vital not only for fostering transparency but also for encouraging a shared sense of responsibility in the maintenance and sustainability of the polder system.

Infrastructure for water management in a polder

The pivotal components of the polder system include ring dikes, an outlet structure (comprising both pumps and gravity outlets), drainage canals, and a retention basin. The construction of ring dikes can be implemented along the catchment boundary of the Bendung River. If all nine sub-catchments are to be developed into polder systems, careful consideration and assessment will be required to design appropriate ring dikes for each system [26].

In areas such as the Bendung sub-catchment, where population density is high and residential land use dominates, accommodating space for retention basins presents a significant challenge. Relocating existing residents is virtually impractical and financially burdensome—an issue similarly faced by other densely populated coastal cities worldwide.

A potential solution to this spatial constraint is the revitalization of urban areas. One approach, as exemplified in Delft, the Netherlands, involves combining vertical housing development with ground-level retention basins. This strategy facilitates runoff storage while simultaneously enhancing the urban landscape. Moreover, it encourages the integration of green spaces and recreational areas into the urban environment, promoting environmental resilience and quality of life. This concept should be explored further in the forthcoming landscape development plan for the lower section of the Bendung area, offering a sustainable and innovative response to flood management challenges in dense urban settings.

The hydraulic analysis in this study was conducted using the Chezy method. The investigation focused on determining the Manning roughness coefficient and the Chezy coefficient in open channels under varying flow discharge conditions, and comparing the obtained roughness coefficients with standard reference values.

A physical model of the channel was constructed for this purpose, with the channel's length and layout designed according to field conditions. The channel slope was maintained at a constant value of 0.01. Discharge values used for the analysis varied and included 0.0025 m^3/s, 0.0022 m^3/s, and 0.0015 m^3/s.

The modeling for this research was carried out using the duFlow program at 75 station (STA) points across the Bendung River system. The cross-section data for the Bendung segment are organized and presented in *Table 3*, with the following subdivisions:

- Part A: STA 1–33
- Part B: STA 34–45
- Part C: STA 46–51
- Part D: STA 52–67
- Part E: STA 68–75

A channel network layout covering five river branches was developed by inputting key data parameters, including rainfall intensity, flow rates, channel dimensions, water levels, boundary velocities, and topographic conditions.

Following the data input, the duFlow simulation was executed. Each simulation graph presents two flow conditions:

- The start condition, representing river flow prior to rainfall events.
- The end condition, representing river flow following rainfall events.

Table 4 presents water level data for Part A. *Figures 8*, *9*, and *10* illustrate the simulation results for the channel, depicting water level, discharge, and flow velocity, respectively.

The results of the duFlow simulation for Part A were analyzed under two conditions:

- Before rainfall at 00:00 hours (baseline condition with no rain), and
- During and after rainfall, beginning at 05:00 hours.

At 05:00, rainfall with an intensity of 59 mm/hour was recorded, causing a rise in water levels along the channel. By 06:00, rainfall intensity increased further to 83 mm/hour, classified as an extreme rainfall event (as shown in *Figure 8*). Rainfall ceased around 11:00, and by 23:50, the river flow had almost returned to normal at most monitoring points, although several locations, particularly between STA 1+000 and STA 2+400, continued to experience elevated water levels.

Based on the analysis presented in *Figure 8*, the simulation shows variations from the highest to the lowest water levels along the channel. Additionally, during the peak event:

- The highest discharge recorded was 78 m^3/s between 05:30 and 06:00 WIB, largely attributed to the operation of the pump located at the weir's mouth.
- The lowest discharge was–23 m^3/s during the same period, indicating the occurrence of localized backflow.

Figure 10 illustrates the variations in flow velocity, depicting both the highest and lowest velocities observed across Part A. At 00:00 (before rainfall), the brown line on the graph represents the elevation of the surrounding land, while the blue line shows the initial water level in Part A, spanning from upstream

(STA 6+400) to downstream (STA 0+000). The average water level along the Bendung River was approximately 17.75 meters during normal conditions.

As rainfall commenced at 05:00, water levels rose significantly, overtopping the adjacent land and resulting in flooding. Flooding was particularly severe between STA 1+000 and STA 2+400. Field surveys conducted in this area identified several causes contributing to the flooding:

- The presence of three low-clearance bridges and PDAM pipelines that restricted water flow.
- The absence of embankments to contain high water levels along this river stretch.
- Discharge from two pumps (Veteran pump and Major Ruslan pump) directly into the Bendung River, which caused turbulence and obstructed natural flow.
- The lowest ground elevation compared to other segments of the river, exacerbating the flood risk.

These factors collectively disrupted river hydraulics, leading to significant localized flooding during the extreme rainfall event.

The water level along Part A at 00:00 is represented by the blue line, while the brown line indicates the elevation of the land along the banks of Part A. The initial conditions at 00:00 show the river profile from upstream (STA 6+400) to downstream (STA 0+000), moving from left to right on the graph. The average water level along the Bendung River under these baseline conditions is approximately 17.75 meters. *Table 3* presents the cross-sectional geometry data for different segments of the Bendung River, divided into five main parts: Part A, Part B, Part C, Part D, and Part E. Each entry in the table corresponds to a specific cross-sectional measurement point (STA), identified by its coordinates (X, Y) and its chainage (STA).

For each cross-section, several key elevation points are recorded:

- Top Left (A) and Top Right (D): Represent the highest points on either bank of the river.
- Bottom Left (B) and Bottom Right (C): Indicate the lowest elevations near the river channel sides.
- Middle Base of the Part (E): Refers to the lowest central point of the channel cross-section, providing critical data for hydraulic modeling.

Additionally, the table includes the channel width (measured in meters) and the maximum depth from the crest to the channel bed at each section. These values are essential for calculating flow area, wetted perimeter, and hydraulic radius, which are key parameters in hydrodynamic simulations using duFlow.

- In Part A, channel widths range roughly from 6 to 23 meters, with depths typically between 2 and 4 meters.
- In Part B and Part C, the channel becomes narrower but deeper in some segments.
- Part D and Part E show more variability in channel width and depth, reflecting changes in river morphology, with certain sections exceeding 5 meters in depth (especially in Part E).

This detailed cross-sectional information provides the geometric foundation for accurately simulating water levels, discharge, and flow velocities during various hydrological conditions in the Bendung River system.

Table 3 Cross-sectional data of the Bendung River channels

Part	No	X	Y	STA	Top Left	Bottom Left	The Middle Base of the Part	Bottom Right	Top Right	Part Width (m)	Depth (m)
					A	B	E	C	D		
Part A	1	474372.000000	9670060.000000	0+000	19.1877	15.144	14.9537	14.9537	19.17	16	4.234
	2	474243.000000	9670210.000000	0+200	19.1617	15.306	15.0207	15.5097	19.14	13	4.141
	3	474097.000000	9670350.000000	0+400	18.4717	16.692	15.0452	16.4737	18.2	13	3.4265
	4	474040.000000	9670490.000000	0+600	18.4077	17.413	14.6377	15.8097	18.32	12	3.77
	5	474007.000000	9670630.000000	0+800	18.3887	17.49	15.5017	16.8697	18.14	11	2.887
	6	474121.000000	9670780.000000	1+000	18.1157	17.001	14.3497	16.8107	18.21	11	3.766
	7	473960.000000	9670860.000000	1+200	18.0157	17.079	14.3497	16.6107	18.42	13	3.666
	8	474043.080481	9670818.003097	1+400	17.9077	16.829	14.6187	16.5277	17.9	10	3.289
	9	473781.000000	9670900.000000	1+600	18.642	16.699	15.7068	16.6087	18.84	10	2.9352

Part	No	X	Y	STA	Top Left	Bottom Left	The Middle Base of the Part	Bottom Right	Top Right	Part Width (m)	Depth (m)
					A	B	E	C	D		
	10	473704.000000	9671030.000000	1+800	18.2281	16.694	15.9618	16.615	18.13	12	2.2663
	11	473679.000000	9671220.000000	2+000	18.034	16.614	15.9618	16.619	18.05	12	2.0722
	12	473610.000000	9671400.000000	2+200	18.213	16.792	15.1128	16.792	18.48	11	3.1002
	13	473533.000000	9671590.000000	2+400	18.136	17.258	15.1128	17.921	18.26	11	3.0232
	14	473409.000000	9671740.000000	2+600	18.486	17.138	15.1128	17.138	18.49	11	3.3732
	15	473365.000000	9671930.000000	2+800	18.772	16.997	16.3438	17.195	18.31	11	2.4282
	16	473309.000000	9672110.000000	3+000	18.517	17.32	15.4248	17.32	18.51	11	3.0922
	17	473294.000000	9672300.000000	3+200	18.343	16.475	15.4248	17.401	18.18	11	2.9182
	18	473264.000000	9672490.000000	3+400	19.142	16.977	15.4248	17.145	19.36	11	3.7172
	19	473274.000000	9672610.000000	3+600	18.454	17.245	15.4248	16.861	19.12	11	3.0292
	20	473210.000000	9672670.000000	3+800	18.908	17.154	15.4248	17.089	18.84	11	3.4832
	21	473020.000000	9672640.000000	4+000	18.526	17.399	15.4248	16.938	18.57	13	3.1012
	22	472822.000000	9672670.000000	4+200	18.387	22.059	15.4248	22.783	23.93	11	2.9622
	23	472636.000000	9672730.000000	4+400	18.366	22.293	16.121	22.543	23.79	11	2.245
	24	472469.000000	9672820.000000	4+600	18.759	17.632	16.121	17.241	18.49	11	2.638
	25	472287.000000	9672880.000000	4+800	18.576	16.717	16.121	16.877	18.51	11	2.455
	26	472156.000000	9672970.000000	5+000	18.603	16.429	16.121	16.756	18.6	12	2.482
	27	472059.000000	9673110.000000	5+200	18.595	17.005	16.875	17.146	18.58	11	1.72
	28	471998.000000	9673300.000000	5+400	19.06	18.268	17.208	17.644	18.38	11	1.852
	29	471896.000000	9673470.000000	5+600	19.249	17.62	17.208	17.467	19.13	11	2.041
	30	471737.000000	9673570.000000	5+800	18.842	17.226	17.208	17.424	18.82	10	1.634
	31	471488.000000	9673880.000000	6+000	18.354	17.354	17.145	18.346	18.53	6	1.209
	32	471341.000000	9674000.000000	6+200	19.105	17.556	17.145	17.417	19.38	6	1.96
	33	471247.000000	9674170.000000	6+400	19.346	17.403	17.145	17.972	19.48	6	2.201
Part B	34	472099.000000	9672830.000000	0+000	18.733	17.556	17.324	17.531	18.76	4	1.409
	35	471903.000000	9672820.000000	0+200	18.215	17.579	17.324	17.887	18.87	4	0.891
	36	471735.000000	9672890.000000	0+400	18.984	18.315	17.823	18.065	19.07	4	1.161
	37	471536.000000	9672900.000000	0+600	19.198	18.657	18.802	18.657	19.9	4	0.396
	38	471339.000000	9672920.000000	0+800	24.043	20.077	19.016	19.09	20.02	2	5.027
	39	471157.000000	9672840.000000	1+000	20.132	19.111	19.047	19.125	19.78	2	1.085
	40	470981.000000	9672750.000000	1+200	20.749	19.728	19.574	20.967	21.62	2	1.175
	41	470760.000000	9672740.000000	1+400	20.473	19.315	19.266	19.121	20.49	2	1.207
	42	470602.000000	9672820.000000	1+600	21.951	20.02	19.92	20.02	21.63	2	2.031
	43	470438.000000	9672790.000000	1+800	20.969	20.707	19.93	20.017	20.65	2	1.039
	44	470289.000000	9672890.000000	2+000	21.072	20.889	20.115	20.898	20.91	2	0.957
	45	470112.000000	9672920.000000	2+200	22.009	21.247	20.751	20.733	21.67	2	1.258
Part C	46	471327.000000	9673080.000000	0+000	20.484	19.784	19.654	19.774	20.48	2	0.83
	47	471188.000000	9673190.000000	0+200	19.755	19.845	19.045	19.845	19.76	2	0.71

Part	No	X	Y	STA	Top Left	Bottom Left	The Middle Base of the Part	Bottom Right	Top Right	Part Width (m)	Depth (m)
					A	B	E	C	D		
	48	471039.000000	9673280.000000	0+400	20.817	20.387	20.157	20.427	20.75	2	0.66
	49	470891.000000	9673380.000000	0+600	22.047	22.117	21.217	21.917	22.05	2	0.83
	50	470755.000000	9673530.000000	0+800	22.533	21.713	21.543	21.683	22.53	2	0.99
	51	470576.000000	9673570.000000	1+000	23.157	22.387	22.227	22.377	23.16	2	0.93
Part D	52	473377.000000	9672700.000000	0+200	18.51	17.138	16.829	17.16	18.45	6	1.681
	53	473426.000000	9672870.000000	0+400	17.806	17.469	16.97	17.806	18.6	6	0.836
	54	473304.000000	9673010.000000	0+600	18.568	17.307	16.81	17.109	18.54	6	1.758
	55	473221.000000	9673170.000000	0+800	18.387	17.134	16.691	17.129	18.5	6	1.696
	56	473246.000000	9673360.000000	1+000	18.57	17.856	16.972	17.484	18.4	6	1.598
	57	473283.000000	9673520.000000	1+200	18.532	17.063	16.773	17.493	18.45	6	1.759
	58	473233.000000	9673720.000000	1+400	19.012	17.298	17.31	16.958	18.51	6	1.702
	59	473196.000000	9673900.000000	1+600	18.651	17.264	16.812	17.137	18.19	6	1.839
	60	473119.000000	9674080.000000	1+800	18.268	17.888	16.865	18.502	19.05	6	1.403
	61	473079.000000	9674270.000000	2+000	18.469	17.373	16.991	17.441	18.72	6	1.478
	62	473138.000000	9674410.000000	2+200	18.923	17.266	16.925	17.366	19.02	6	1.998
	63	473255.000000	9674520.000000	2+400	18.397	17.52	17.645	17.77	19.07	6	0.752
	64	473328.000000	9674660.000000	2+600	19.412	17.98	17.249	17.913	19.3	6	2.163
	65	473407.000000	9674840.000000	2+800	19.194	17.85	17.821	17.799	19.06	6	1.373
	66	473573.000000	9674920.000000	3+000	19.685	18.563	17.829	18.845	19.74	6	1.856
	67	473747.000000	9675010.000000	3+200	19.757	18.751	18.68	18.697	19.88	6	1.077
Part E	68	474120.000000	9671000.000000	0+200	21.0124	18.477	18.024	19.15	21.16	7	2.9884
	69	474130.000000	9671190.000000	0+400	21.0124	18.477	18.285	19.15	21.16	7	2.7274
	70	474094.000000	9671380.000000	0+600	21.0124	18.477	15.748	19.15	21.16	4	5.2644
	71	474173.000000	9671550.000000	0+800	21.0124	18.477	16.071	19.15	21.16	2	4.9414
	72	474144.000000	9671720.000000	1+000	21.0124	18.477	15.939	19.15	21.16	2	5.0734
	73	474158.000000	9671890.000000	1+200	21.0124	18.477	16.198	19.15	21.16	2	4.8144
	74	474092.000000	9671990.000000	1+400	21.0124	18.477	19.084	19.15	21.16	2	1.9284
	75	474025.000000	9672150.000000	1+600	21.0124	18.477	18.132	19.15	21.16	2	2.8804

Table 4 Water level data for part A

STA	Surface level	Water level				
		0.00	5.00	11.00	11.00	23.50
6+400	19.346	17.8	17.86	19.77	18.6	18.1
6+200	19.105	17.8	17.86	19.77	18.6	18.1
6+000	18.354	17.8	17.87	19.77	18.6	18.1
5+800	18.842	17.8	17.91	19.77	18.6	18.1
5+600	19.249	17.8	17.97	19.77	18.6	18.1
5+400	19.06	17.8	18.02	19.77	18.6	18.1
5+200	18.595	17.8	18.06	19.78	18.6	18.1
5+000	18.603	17.7	18.09	19.78	18.6	18.1
4+800	18.576	17.7	18.11	19.78	18.6	18.1
4+600	18.759	17.7	18.12	19.78	18.6	18.1

STA	Surface level	Water level				
		0.00	5.00	11.00	11.00	23.50
4+400	18.36	17.7	18.13	19.79	18.6	18.1
4+200	18.38	17.7	18.14	19.79	18.6	18.1
4+000	18.526	17.7	18.16	19.79	18.6	18.1
3+800	18.908	17.7	18.15	19.77	18.6	18.1
3+600	18.454	17.8	18.14	19.71	18.6	18.1
3+400	19.142	17.8	18.14	19.69	18.6	18.1
3+200	18.343	17.8	18.14	19.67	18.6	18.1
3+000	18.517	17.8	18.16	19.65	18.6	18.1
2+800	18.772	17.8	18.18	19.6	18.6	18.1
2+600	18.486	17.8	18.18	19.58	18.6	18.1
2+400	18.136	17.8	18.18	19.56	18.6	18.1
2+200	18.213	17.8	18.2	19.54	18.6	18.1
2+000	18.034	17.8	18.22	19.51	18.6	18.1
1+800	18.2281	17.7	18.25	19.49	18.6	18.1
1+600	18.642	17.7	18.29	19.46	18.6	18.1
1+400	17.9077	17.7	18.37	19.44	18.6	18.1
1+200	18.0157	17.7	18.4	19.42	18.6	18.1
1+000	18.1157	17.7	18.3	19.31	18.6	18.1
0+800	18.3887	17.7	18.14	19.04	18.6	18.1
0+600	18.4077	17.7	18.02	18.9	18.6	18.1
0+400	18.4717	17.7	17.97	18.74	18.6	18
0+200	19.1617	17.7	17.71	17.75	18.6	18
0+000	19.1877	17.7	17.71	17.73	18.6	18

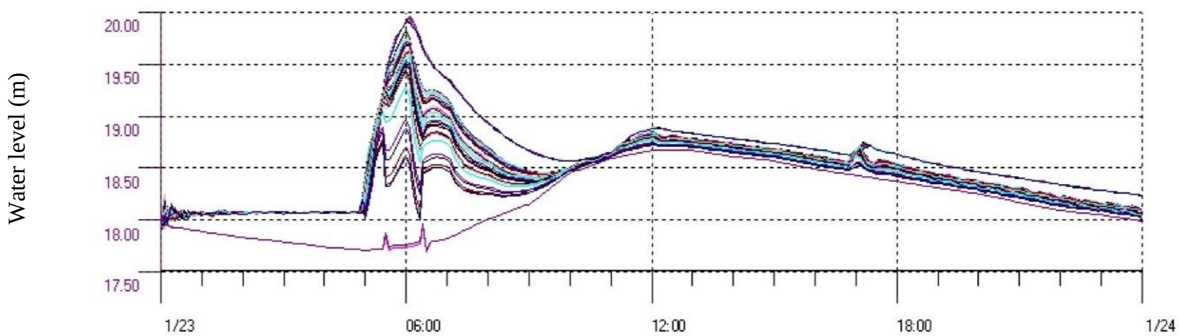

Figure 8 Water level graph on channel 1

At 05:00, rainfall began with an intensity of 59 mm/hour. Observations indicated that the water level exceeded the land elevation at several points, resulting in flooding. The flooded area was identified between STA 1+000 and STA 2+400. A field survey of the existing conditions at the Bendung River revealed several factors contributing to the flooding at this location:

- The presence of three low-clearance bridges and PDAM pipelines, which obstructed the natural flow of the river.
- The absence of embankments along this river segment, allowing water to overflow onto adjacent lands.
- The operation of two pumps—the Veteran pump and the Major Ruslan pump—which discharge water directly into the Bendung River. This discharge created turbulence that further hindered smooth flow and exacerbated the flooding conditions.

Additionally, this segment of the river has the lowest elevation compared to other areas along the Bendung River, making it particularly vulnerable to overflow and inundation during periods of heavy rainfall.

The water level graph shown in *Figure 8* illustrates the variations in channel water levels over time. Initially, the water level remained relatively constant. However, at 05:00, the graph shows a sharp rise, coinciding with the onset of heavy rainfall. At 06:00, the water level began to gradually decline, and by

11:00, the rainfall had ceased, allowing the water level to stabilize. Rainfall resumed briefly at 12:00, causing a slight increase in the water level once again. Following a two-hour period without rain from 13:00 to 14:00, the graph indicates a decline in the water level. At 17:00, the graph shows another noticeable rise as rainfall resumed. After 19:00, as the rain diminished, the water level gradually decreased again, reflecting the cessation of rainfall.

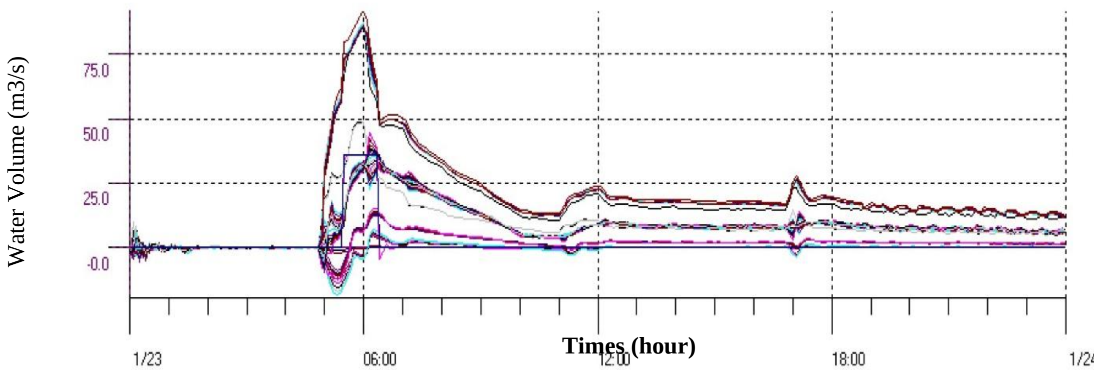

Figure 9 Discharge graph on channel

The discharge graph shown in *Figure 9* presents the variation in water discharge over time based on the channel modeling results. The graph indicates that between 05:00 and 06:00, the water discharge peaked at 78 m³/s, primarily due to the very high rainfall intensity during that period. The highest discharge values were observed downstream, where a pump with a capacity of 36 m³/s, supported by a sluice gate, helped manage the flow.

Following this peak, the discharge gradually declined until around 10:00, corresponding with a decrease in rainfall intensity. A secondary rise in discharge occurred around 12:00, triggered by the resumption of rainfall. Between 13:00 and 17:00, the water discharge remained relatively constant. However, the graph shows another slight increase starting at 18:00, linked to another rainfall event. Despite the rain, the discharge slightly decreased around 17:30, likely due to the lower intensity of the rainfall at that time.

Based on these observations, the data suggest that the existing drainage infrastructure may not be fully adequate to accommodate extreme discharge events. This highlights the urgent need for infrastructure improvements and enhanced flood management measures to better cope with high-intensity stormwater events.

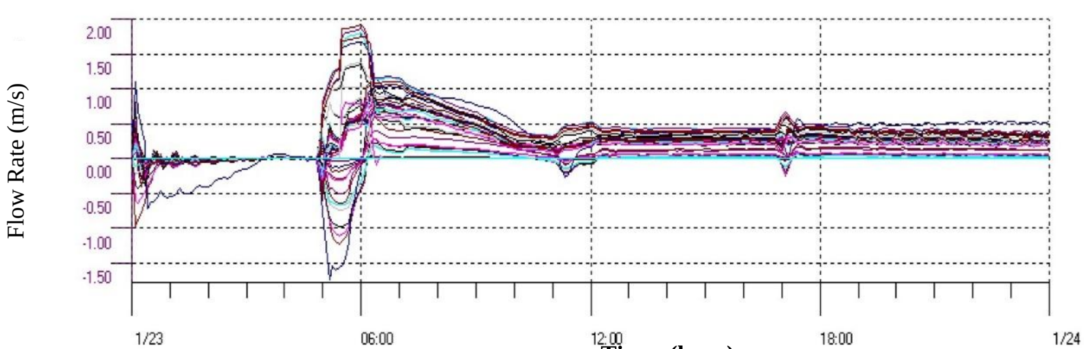

Figure 10 Velocity graph on channel

The flow velocity graph presented in *Figure 10* illustrates the changes in water velocity within the channel over time. The graph shows that the flow velocity began to increase at 05:00, coinciding with the onset of rainfall. Although rainfall continued until 11:00, the flow velocity began to gradually decrease after 06:00, as the rainfall intensity lessened compared to the initial surge between 05:00 and 06:00.

At 11:00, the graph stabilizes, indicating that the rainfall had stopped and the flow velocity became relatively constant. Rainfall resumed at 12:00, causing a subsequent increase in flow velocity. However, after this brief event, the flow velocity again stabilized as rainfall ceased between 13:00 and 17:00.

A final increase in velocity is observed after 17:00, corresponding to another rainfall event, with flow velocity continuing to rise until approximately 18:00 before stabilizing once the rainfall diminished.

At 06:00, the rainfall intensity peaked at 83 mm/hour, resulting in a sharp rise in water levels to approximately 19.75 meters, as shown in the graphs. Almost all locations in Part A were affected by flooding. The flooding occurred because the river system was unable to accommodate the high volume of rainfall.

Several factors contributed to this situation:

- The presence of low-clearance bridges and PDAM pipelines that obstructed the natural flow of water.
- Severe sedimentation in certain areas, especially near STA 5+800 to STA 6+000 where the Talang Aman Retention Pond is located; the pond has become shallow over time.
- A sluice gate located in this area was found to be non-functional.
- Most stretches of Part A lack embankments, allowing water to overflow directly onto adjacent land during heavy rainfall.

Even after the rain had stopped at 11:00, flooding persisted at several locations. This is evident from *Figure 10*, where water levels still exceeded the land boundary at many points. Areas still inundated include:

- The Talang Aman Retention Pond Area (STA 5+800 to 6+000),
- The Lebak Rejo riverbank area (STA 4+000 to STA 4+800),
- The Sekip Bendung and Jalan Gersik areas (STA 3+600 to STA 3+800),
- Other critical points previously identified.

By 23:50, water levels had reduced but remained elevated at an average height of 18.10 meters, with minor flooding still observed, albeit lower compared to the peak event.

The water level remained stable before 05:00 but showed a sharp increase when heavy rainfall began (*Figure 8*). After peaking at 06:00, the level gradually declined as rainfall intensity lessened and eventually stopped around 11:00. Another minor increase occurred after rainfall resumed at 12:00, followed by stabilization during the rain-free period from 13:00 to 17:00. A final rise in water levels occurred after 17:00 due to renewed rainfall, before gradually declining again after 19:00.

Between 05:00 and 06:00, water discharge peaked at 78 m^3/s (*Figure 9*). This high discharge was due to intense rainfall and was most significant downstream, where a 36 m^3/s pump and a sluice gate were operating. Following the peak, discharge steadily declined by 10:00 as rainfall intensity decreased. A secondary increase occurred around 12:00, after which discharge remained stable from 13:00 to 17:00. Another minor discharge spike appeared at 18:00, although lower rain intensity caused a slight decrease around 17:30.

Flow velocity increased starting at 05:00 due to heavy rainfall, then began a gradual decline after 06:00 as rainfall intensity dropped (*Figure 10*). After 11:00, when the rain stopped, the velocity stabilized. Another slight increase was observed around 12:00 with renewed rainfall, followed by a relatively constant velocity until 17:00. After renewed rain at 17:00, the velocity rose again, peaking around 18:00.

Channel 1 of the Bendung River was modeled using the duFlow Modelling Studio, with a network of 33 nodes from STA 0+000 (near the Musi River) to STA 6+400 upstream.

Similarly, [28] modeled the Aur Sub-Catchment (Palembang, South Sumatra) using 44 nodes, concluding that installing a 12 m^3/s pump in the downstream section significantly reduced inundation. The findings of this study align with those of the Aur Sub-Catchment study, confirming that increasing pump capacity can be an effective flood mitigation strategy.

Based on these findings, it is recommended that the Palembang City Government:

- Tighten residential development permits along rivers and canals to prevent further land-use changes that increase flood vulnerability.
- Strengthen urban planning policies by protecting natural drainage paths and incorporating flood risk assessments into development plans.

Failure to manage residential growth along waterways risks exacerbating future flooding incidents.

The study demonstrates that high rainfall intensity significantly affects water level, discharge, and flow velocity in the Bendung River system. The channel infrastructure, as currently configured, is inadequate to accommodate extreme storm events, particularly around vulnerable locations like Talang Aman. Even after rainfall cessation, floodwaters persisted in several areas, emphasizing the limited drainage capacity of the existing system and the urgent need for upgrades. Comparisons with the Aur Sub-Catchment study reveal similar patterns of flood occurrence due to insufficient drainage capacity. The successful mitigation there—achieved by installing higher-capacity pumps—suggests that infrastructure upgrades and increased pumping capacity could significantly reduce flood risks in Palembang.

Study limitations

While the analysis provides a clear overview of the relationship between rainfall and flooding, there are several limitations to this study. One major limitation is the use of the duFlow model, which, although capable of simulating hydrological variables, does not fully account for other critical factors such as land-use changes and the long-term impacts of climate change. Additionally, limitations in the availability and quality of channel data and physical parameters used in the simulation may have affected the accuracy of the results. Future research that incorporates a broader range of variables and more extensive field data is recommended to produce a more comprehensive and reliable assessment.

Future scope

Future studies should focus on:

1. Long-Term Hydrological Modeling: Simulate seasonal and climate-change-induced rainfall variations.
2. Pump and Infrastructure Optimization: Analyze pump sizing and operation for different rainfall scenarios.
3. Urban Development Impact Analysis: Assess how residential expansion affects flood vulnerability.
4. Flood Mitigation Strategies: Investigate green infrastructure solutions like wetlands, retention ponds, and embankments.
5. Advanced Modeling Techniques: Incorporate machine learning or artificial intelligence to improve predictive flood modeling and management.

By pursuing these areas, future research can offer targeted, resilient, and adaptive solutions for urban flood risk management in Palembang and similar coastal cities.

A complete list of abbreviations is listed in *Appendix I*.

5.Conclusion

The research findings indicate that developing a polder system in the Bendung sub-basin is a feasible and effective solution for controlling runoff and mitigating floods. The construction of ring dikes can be aligned with the existing road network along the sub-catchment boundary, offering a practical and cost-efficient approach. However, careful evaluation of the interaction between the Bendung polder and the surrounding eight sub-basins is necessary to prevent negative hydraulic impacts on adjacent areas. The pumping system currently operating at the mouth of the Bendung River should be further optimized to manage floodwaters efficiently, with particular attention to assessing the hydraulic response during pump operation to avoid sudden water depletion. It is also essential to establish a clear, practical, and easy-to-follow operational protocol for the polder and pumping system to ensure effective management. Given the dense land use along the riverbanks, normalizing the river profiles is not a viable option, emphasizing the need for alternative flood protection measures. Furthermore, enhancing solid waste management is critical to the success of flood mitigation efforts. Training and community engagement programs should be incorporated to promote proper waste handling and maintain the functionality of drainage and polder systems over the long term.

Acknowledgment

The author would like to express sincere gratitude for the support and valuable contributions from all parties who assisted throughout the research process. The success of this study would not have been possible without the guidance, suggestions, and constructive input generously provided by various individuals and institutions.

Conflicts of interest

The authors have no conflicts of interest to declare.

Data availability

All data supporting the findings of this study are available from the corresponding author upon reasonable request. The data have been anonymized to protect the privacy of individuals.

Authors contribution statement

Marlina Sylvia: Conceptualization, data analysis, writing – original draft, writing – review and editing. **Anis Saggaff:**

Methodology, validation, formal analysis. **F.X. Suryadi:** Methodology, validation, formal analysis.

References

[1] Istianto H, Bernard R, Suryadi FX. Improving the performance of tidal irrigation through the water management, (study case Gandus Palembang, South Sumatra). In proceedings–international association for hydro-environment engineering and research (IAHR)-Asia Pacific division (APD) congress: multi-perspective water for sustainable development 2018 (pp. 677-85).

[2] Istianto HA, Suryadi F, Hamim S. Potentials and constraints of urban polder development in Jakarta, Indonesia, case study: Rawa Badak polder. In proceedings of the 37th IAHR world congress, Malaysia 2017 (pp.1-8).

[3] Hein C. Adaptive strategies for water heritage: past, present, and future. Springer Nature; 2020.

[4] David A, Schmalz B. Flood hazard analysis in small catchments: comparison of hydrological and hydrodynamic approaches by the use of direct rainfall. Journal of Flood Risk Management. 2020; 13(4):1-26.

[5] De SDC, Engel VL. Direct seeding reduces costs, but it is not promising for restoring tropical seasonal forests. Ecological Engineering. 2018; 116:35-44.

[6] Dalhuisen JM, Rodenburg CA, De Groot HL, Nijkamp P. Sustainable water management policy: lessons from Amsterdam. European Planning Studies. 2003;11(3):263-81.

[7] Khan MS, Paul SK. Fresh water management in coastal Bangladesh: preparedness and adaptation. Discover Water. 2023; 3(1):27.

[8] Pujiastuti R. The initial step for developing sustainable Urban Drainage system in semarang city-Indonesia. Procedia Engineering. 2017; 171:1486-94.

[9] Hashemi F, Olesen JE, Jabloun M, Hansen AL. Reducing uncertainty of estimated nitrogen load reductions to aquatic systems through spatially targeting agricultural mitigation measures using groundwater nitrogen reduction. Journal of Environmental Management. 2018; 218:451-64.

[10] Baransi-karkaby K, Hassanin M, Muhsein S, Massalha N, Sabbah I. Innovative ex-situ biological biogas upgrading using immobilized biomethanation bioreactor (IBBR). Water Science and Technology. 2020; 81(6):1319-28.

[11] Miguez MG, Veról AP, De Sousa MM, Rezende OM. Urban floods in lowlands—levee systems, unplanned urban growth, and river restoration alternative: a case study in Brazil. Sustainability. 2015; 7(8):11068-97.

[12] Romano O, Akhmouch A. Water governance in cities: current trends and future challenges. Water. 2019; 11(3):1-9.

[13] Yulianti, Goulter I. Investigation of improvement of the pluit polder system to reduce flooding in Jakarta, Indonesia. In international symposium on urban stormwater management 1992 (pp. 378-83). Barton, ACT: Institution of Engineers, Australia.

[14] Jensen O, Nair S. Integrated urban water management and water security: a comparison of Singapore and Hong Kong. Water. 2019; 11(4):1-18.

[15] Nath S, Dunn FE, Van LF, Driessen PP. Coping with crisis on the coast: the effect of community-developed coping-strategies on vulnerability in crisis-prone regions of the Ganges delta. Journal of Environmental Management. 2021; 284(2021):1-12.

[16] Nath S, Van LF, Driessen PP. Have Bangladesh's polders decreased livelihood vulnerability? a comparative case study. Sustainability. 2019; 11(24):1-20.

[17] Vergroesen AJ, Van DGNC, Van DVFH. Comparison of implicit and explicit connection of fast-and slow-flowing components of a water system. Hydrological Sciences Journal. 2010; 55(3):287-302.

[18] Wignyosukarto BS, Mawandha HG, Jayadi R. Mini polders, as an alternative of flood management in the lower Bengawan solo river. Irrigation & Drainage Systems Engineering. 2015; 4(131):72-80.

[19] Walski T, Creaco E. Selection of pumping configuration for closed water distribution systems. Journal of Water Resources Planning and Management. 2016; 142(6):04016009.

[20] Maryam M, Kumar R, Thahaby N. Assessment of the hydraulic performance of the urban drainage system due to climate change using DHI MIKE URBAN. Journal of Biomedical Research & Environmental Sciences. 2021; 2(4):261-7.

[21] Suryadi FX. Hydraulic performance of urban polder water management and flood protection systems in Jakarta. In conference paper of 13th international conference in urban drainage 2014 (pp.1-8).

[22] Rodríguez JP, Diaz-granados MA, Rodríguez MS, Fonseca SA, Mestra GL, Penagos JC, et al. Integrated management and modelling in urban drainage systems: the potentialities in a developing megacity. In 8th world wide workshop for young environmental scientists: urban waters: resource or risks? 2009 (pp. 1-13). HAL Open Science.

[23] Hellmers S, Fröhle P. Computation of backwater effects in surface waters of lowland catchments including control structures–an efficient and re-usable method implemented in the hydrological open-source model Kalypso-NA (4.0). Geoscientific Model Development. 2022; 15(3):1061-77.

[24] Zareef L, Jalali M, Sadat SM. Analysis of the potential for use of floating solar panels on Naghlo hydropower dam. International Journal of Innovative Research and Scientific Studies. 2021; 4(2):126-32.

[25] Singhal S, Srivastava AK. Study of rainfall induced landslide with different slope profile. In AIP conference proceedings 2024. AIP Publishing.

[26] Kalmah L, Suryadi FX, Schultz E. Evaluation of urban polder drainage system performance in Jakarta. case study Kelapa Gading area. The 6th Asian regional conference of ICID of international commission on irrigation and drainage, Yogyakarta 2010.

[27] Prabnakorn S, Suryadi FX, Chongwilaikasem J, De FC. Development of an integrated flood hazard

assessment model for a complex river system: a case study of the Mun River Basin, Thailand. Modeling Earth Systems and Environment. 2019; 5(4):1265-81.
[28] Fraiture CD, Susanto RH, Suryadi FX, Wahyu HM. Urban drainage management and flood control improvement using the duflow case study: aur sub catchment, Palembang, south Sumatra, Indonesia. Makara Journal of Technology. 2017; 21(2):83-92.

Marlina Sylvia is a Ph.D. student in the Civil Engineering and Planning Department, Faculty of Engineering, Universitas Sriwijaya, Indonesia. Her research interests include Water Irrigation, Drainage, Land Use Planning, Polder Systems, and Flood Management.
Email: marlinas3@gmail.com

Anis Saggaff is a professor and lecturer in the Civil Engineering and Planning Department, Faculty of Engineering, Universitas Sriwijaya, Indonesia. He received his Doctorate in Civil Engineering from Universiti Teknologi Malaysia in 2007. His research focuses on Steel Structures, Steel Composites, Self-Compacting Concrete, Geopolymer Concrete, and Lightweight Concrete.
Email: anissaggaf@yahoo.com

F.X. Suryadi is a senior lecturer at the IHE Delft Institute for Water Education (UNESCO-IHE), Department of Water Science and Engineering, South Holland, Netherlands. His research focuses on Water Irrigation, Drainage, Land Use Planning, Polder Systems, Climate Change, and Agriculture.
Email: suryadi.ihe@gmail.com

Appendix I

S. No.	Abbreviation	Description
1	BMKG	Badan Meteorologi, Klimatologi, dan Geofisika (Meteorology, Climatology, and Geophysics Agency)
2	IDF	Intensity-Duration-Frequency
3	STA	Station